Available online at www.sciencedirect.com
ScienceDirect
Journal of Catalysis 247 (2007) 78–85
JOURNAL OF CATALYSIS
www.elsevier.com/locate/jcat

Effect of boron addition on the surface structure of $Co\text{-}Mo/Al_2O_3$ catalysts

Usman, Takeshi Kubota, Ichiro Hiromitsu, Yasuaki Okamoto *

Department of Material Science, Shimane University, Matsue 690-8504, Japan

Received 11 October 2006; revised 13 January 2007; accepted 17 January 2007

Available online 16 February 2007

Abstract

The effect of boron addition was studied on the surface structure of $Co\text{-}MoS_2/Al_2O_3$ catalysts prepared by an impregnation technique. A chemical vapor deposition (CVD) technique using $Co(CO)_3NO$ was applied to evaluate the maximum potential hydrodesulfurization (HDS) activity of the catalysts, the extent of blocking of MoS_2 edges by cobalt sulfides, and the coverage of Co on the MoS_2 edges. The catalysts were characterized by means of UV–vis spectroscopy and magnetic susceptibility measurements. The addition of boron decreased the catalytic activity of $Co\text{-}MoS_2/Al_2O_3$ for the HDS of thiophene, irrespective of calcination and Co loading. However, the extent of increased HDS activity of $Co\text{-}MoS_2/Al_2O_3$ from the addition of Co using the CVD technique was greater for the boron-containing catalysts than for the corresponding boron-free catalysts. Characterization by the CVD technique showed that boron significantly increased the extent of blocking and decreased the Co coverage on MoS_2 edges. The surface structure of uncalcined $Co\text{-}MoS_2/Al_2O_3$ catalysts estimated by use of the CVD technique was substantiated by the magnetic property of Co.

Keywords: Hydrodesulfurization; $Co\text{-}Mo/Al_2O_3$; Effect of boron; Surface structure; Magnetic properties of Co

1. Introduction

The quality of crude oil has been decreasing year by year, resulting in a reduced yield of straight-run fractions of fuel oils. Meanwhile, increasingly stringent environmental regulations that limit the amounts of sulfur and aromatics in fuel are being put into effect [1–3]. This has forced refineries to seek new technologies to convert heavier fractions to high-quality products, resulting in an increasing attention to hydrodesulfurization (HDS) catalysts. Sulfided Mo- or W-based catalysts have been widely used for industrial HDS reactions [4–7].

Topsøe and co-workers [5,8,9] have proposed that the catalytically active phase in promoted Co(Ni)-Mo sulfide catalysts is the so-called Co(Ni)-Mo-S phase, in which Co(Ni) atoms are located on the edge of MoS_2 particles. Based on the intrinsic catalytic activity, they have shown that there are two types of the Co-Mo-S phase: Co-Mo-S type I and Co-Mo-S type II [5,8,9]. Although the origin of the two types of the Co-Mo-S phase remains under debate [10], it is suggested that the Co-Mo-S type I is related to highly dispersed single slab MoS_2 particles maintaining their interactions with the support (e.g., Mo-O-Al bonds), whereas Co-Mo-S type II is related to MoS_2 particles mainly stacked and not linked to the support. The intrinsic HDS activity of the latter phase is more than twice as high as that of the former phase [5,8,9,11].

The addition of boron to Al_2O_3 has been reported to improve the performance of Ni(Co)-promoted molybdenum sulfide catalysts for hydrodenitrogenation (HDN) [12–14], hydrocracking [12], and HDS [12,15–17]. Contradictory results also have been reported, however; for example, Lewandowski and Sarbak [13] reported that the addition of boron did not affect the activity of $Ni\text{-}Mo/Al_2O_3$ catalysts for the HDS of coal liquid.

The role of boron in improving the performance of HDS catalysts is not clearly understood at present. It has been widely reported that increased acidity of boron-modified alumina improves catalyst performance [12–14]; however, on the basis of our detailed characterizations using a $Co(CO)_3NO$-CVD technique of boron-added $CoMo/Al_2O_3$ catalysts [17,18], we have

* Corresponding author.
E-mail address: yokamoto@riko.shimane-u.ac.jp (Y. Okamoto).

0021-9517/$ – see front matter
doi:10.1016/j.jcat.2007.01.010

concluded that the addition of boron improves catalyst performance by weakening the surface interactions between molybdenum oxides and the Al_2O_3 surface, thus leading to a shift of the type of the active sites from a less active Co-Mo-S type I to a more active Co-Mo-S (pseudo) type II. The weakened interactions between Mo species and the Al_2O_3 surface concomitantly resulted in a decrease in the dispersion of Mo in Mo/Al_2O_3 catalysts, in agreement with Morishige and Akai [19]. However, the effect of boron addition on the chemical state of Co on a Co-MoS_2/Al_2O_3 catalyst has rarely been reported. Stranick et al. [20] showed by XPS, ISS, and DRS UV–vis investigation that the addition of boron to Al_2O_3 improved the dispersion of Co and modified the chemical state of Co in Co/Al_2O_3 catalysts. However, no literature has reported the effect of boron addition on the surface structure of Co-Mo catalysts (i.e., the coverage of Co on MoS_2 edges and the blocking of MoS_2 edges by catalytically inactive cobalt sulfide clusters), despite the fact that these pieces of information are of great importance in understanding the nature of the additive. On the basis of comprehensive knowledge of the role of boron in Co-Mo/B_2O_3-Al_2O_3 catalysts, highly active Co-Mo catalysts could be generated by a proper preparation technique.

In our previous studies [21–24], we showed that when a supported Mo sulfide catalyst is exposed to a vapor of $Co(CO)_3NO$ (CVD-technique), followed by evacuation and resulfidation, the Co species in the resultant CVD-Co/MoS_2 catalyst are selectively transformed into the Co-Mo-S phase, and, accordingly, the amount of Co in the catalyst represents the amount of the Co-Mo-S phase. In the CVD-Co/MoS_2 catalysts, the edge of MoS_2 particles can be fully covered by the Co-Mo-S phase [21–24]. Therefore, the CVD technique is a powerful technique for investigating the maximum potential activity of a Co-Mo catalyst and the Co coverage and blocking of MoS_2 edges. In the present study, through a chemical vapor deposition (CVD) technique using $Co(CO)_3NO$, we investigated the effect of boron addition and calcination on the surface structure of Co-Mo/Al_2O_3 catalysts. We show that the addition of boron increases the extent of blocking and decreases the Co coverage on MoS_2 edge sites.

2. Experimental

2.1. Catalyst preparation

MoO_3/B_2O_3-Al_2O_3 was prepared by a double-impregnation technique [17,25]. First, γ-Al_2O_3 (Nikki Chemical Co.; 180 $m^2\,g^{-1}$) was impregnated with an H_3BO_3 aqueous solution (0.6 wt% B), followed by calcination at 773 K for 5 h. Then the B_2O_3-Al_2O_3 material, denoted as BAl, was impregnated with an aqueous solution of $(NH_4)_6Mo_7O_{24}\cdot 4H_2O$ (13 wt% MoO_3) and calcined again at 773 K for 5 h. This catalyst is designated MoO_3/BAl. Similarly, a MoO_3/Al_2O_3 catalyst was prepared by impregnating Al_2O_3 with an aqueous solution of $(NH_4)_6Mo_7O_{24}\cdot 4H_2O$ (13 wt% MoO_3) and subsequent calcination at 773 K for 5 h; the resulting catalyst is designated MoO_3/Al.

Two series of CoO-MoO_3/BAl and CoO-MoO_3/Al catalysts (Co content 1–10 wt%; B content fixed at 0.6 wt% with respect to Al_2O_3) were prepared by impregnating MoO_3/BAl and MoO_3/Al, respectively, with an aqueous solution of $Co(NO_3)_2\cdot 6H_2O$. After impregnation, the catalysts were dried at 383 K for 16 h and then calcined in air at 773 K for 5 h. An aliquot of the catalyst remained uncalcined. Another series of CoO-MoO_3/BAl catalysts, in which the Co content was fixed at 4 wt% and the B content was varied between 0.3 and 4.7 wt%, was prepared in a similar way by impregnating MoO_3/BAl with an aqueous solution of $Co(NO_3)_2\cdot 6H_2O$. The catalysts were subjected to calcination at 773 K for 5 h.

The prepared catalysts were presulfided in a 10% H_2S/H_2 stream at 673 K for 1.5 h. The Mo sulfide catalysts with and without the addition of boron are designated MoS_2/BAl and MoS_2/Al, respectively. The Co-Mo sulfide catalysts are denoted as Co-MoS_2/BAl (with B addition) and Co-MoS_2/Al (without B addition), followed by cal or unc in parentheses, if necessary, for the catalysts calcined or uncalcined after the impregnation of Co. For example: Co-MoS_2/BAl(unc) means a sulfided Co-Mo catalyst supported on B_2O_3-Al_2O_3 without calcination (just dried) after the impregnation of Co.

The sulfided catalysts (MoS_2/BAl, MoS_2/Al, Co-MoS_2/BAl, and Co-MoS_2/Al) were evacuated at 673 K for 1 h before being exposed to a vapor of $Co(CO)_3NO$ at room temperature (CVD technique) [21–23]. After evacuation at room temperature, the catalysts were sulfided again at 673 K for 1.5 h to prepare Co-Mo sulfide catalysts. The catalysts thus prepared using $Co(CO)_3NO$ were designated CVD-Co/MoS_2/BAl when MoS_2/BAl was used and CVD-Co/Co-MoS_2/BAl when Co-MoS_2/BAl was subjected to the CVD procedure. The amount of Co incorporated by the CVD technique was determined for the sulfided catalyst by means of XRF (Shimadzu, EDX-700HS).

2.2. Reaction procedure

The initial activities of the freshly prepared catalysts were evaluated at 623 K for the HDS of thiophene using a circulation reaction system made of glass under mild reaction conditions (initial hydrogen pressure, 20 kPa), after evacuation at 673 K for 1 h. The pressure of thiophene was kept constant (2.6 kPa) during the reaction. The HDS activities were calculated on the basis of the accumulated amount of H_2S. The details of the reaction procedure have been reported previously [21].

2.3. UV–vis spectra

DRS UV–vis spectra of CoO-MoO_3/Al and CoO-MoO_3/BAl were collected in air on a UV-2500PC spectrometer (Shimadzu), in a wavelength range 240–850 nm, using $BaSO_4$ powder as a reference. The sample was diluted in $BaSO_4$ (1:5).

2.4. Magnetic properties

The static magnetic susceptibility measurements of the sulfided catalysts were done in situ with a Faraday method using a

Cahn 2000 Electro-Balance system at 4.2–300 K [26]. The catalyst samples were evacuated at 673 K for 1 h before being fused into a quartz tube. The magnitude of the magnetic field was fixed at 10,000 G. The effective magnetic moment and magnetic susceptibility were obtained by subtracting the magnetic contributions of the quartz ampoule and MoS_2/Al measured separately under identical conditions. The catalyst sample was Co-MoS_2/Al(unc) (Co content: 0.77, 1.54, 2.31, and 3.08 wt%).

3. Results

3.1. HDS activity of Co-MoS_2/(B_2O_3)-Al_2O_3 catalysts

Fig. 1 depicts the HDS activity of the Co-MoS_2 catalysts as a function of boron loading. The HDS activity of Co-MoS_2/(B)Al(cal) was not changed by the addition of 0.3 wt% B, but gradually decreased with a further increase in boron content. Addition of Co to Co-MoS_2/BAl by the CVD technique (CVD-Co/Co-MoS_2/BAl) led to a significant increase in HDS activity. As for CVD-Co/Co-MoS_2/BAl(cal), HDS activity was slightly increased by the addition of boron up to 0.6 wt% B, then decreased on further addition of boron. The maximum activity of CVD-Co/MoS_2/BAl(cal) was attained at 0.3–0.6 wt% B, in agreement with a previous study [17]. As shown in Fig. 1, the HDS activity of the catalysts decreased in the order CVD-Co/MoS_2/(B)Al(cal) > CVD-Co/Co-MoS_2/(B)Al(cal) > Co-MoS_2/(B)Al(cal) over the whole range of boron loading.

The HDS activity of Co-MoS_2/Al(cal) increased as Co loading was increased up to ca. 4 wt%, then slightly decreased with a further increase (Fig. 2). The HDS activity was marginally decreased by the addition of 0.6 wt% B (Co-MoS_2/BAl), as shown in Fig. 2. The addition of Co to Co-MoS_2/Al and Co-MoS_2/BAl by CVD enhanced the HDS activity of these catalysts; the increase was more significant for Co-MoS_2/BAl than for the counterpart without boron.

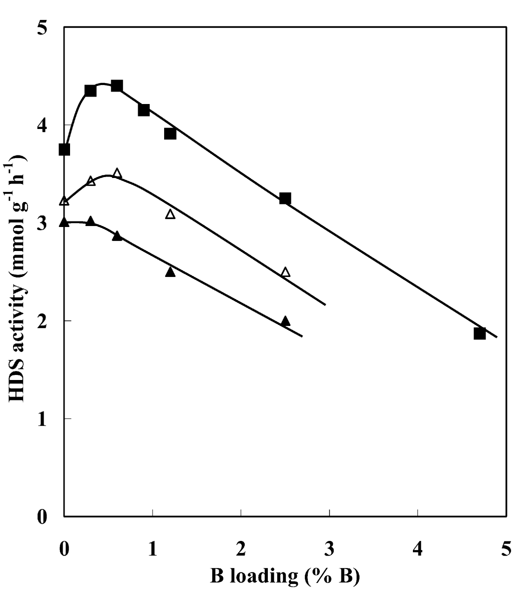

Fig. 1. HDS activity of the Co-MoS_2 catalyst as a function of B loading. (▲) Co-MoS_2/BAl(cal) (4 wt% Co), (△) CVD-Co/Co-MoS_2/BAl(cal) (4 wt% Co), (■) CVD-Co/MoS_2/BAl.

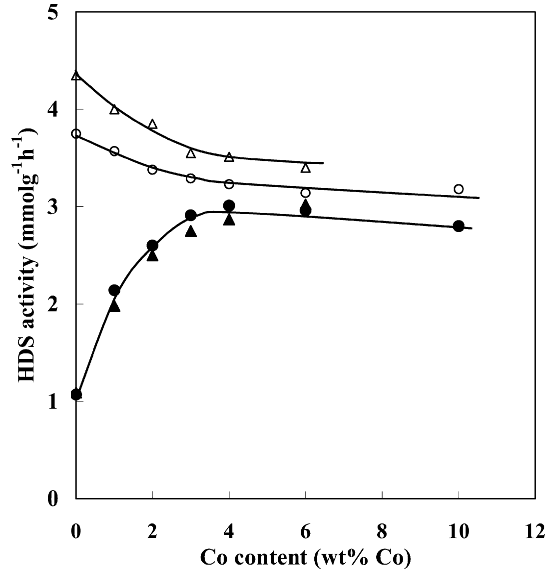

Fig. 2. HDS activity of the Co-MoS_2 catalyst as a function of Co content. (●) Co-MoS_2/Al(cal), (▲) Co-MoS_2/BAl(cal) (0.6 wt% B), (○) CVD-Co/Co-MoS_2/Al(cal), (△) CVD-Co/Co-MoS_2/BAl(cal) (0.6 wt% B). The catalyst was calcined after every step of the impregnation.

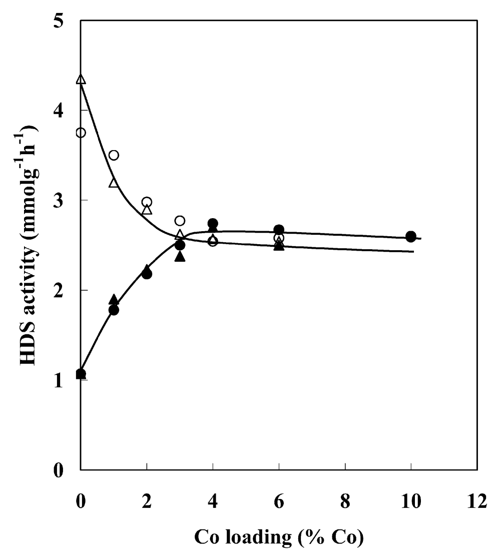

Fig. 3. HDS activity of the Co-MoS_2 catalyst as a function of Co loading. (●) Co-MoS_2/Al(unc), (▲) Co-MoS_2/BAl(unc) (0.6 wt% B), (○) CVD-Co/Co-MoS_2/Al(unc), (△) CVD-Co/Co-MoS_2/BAl (unc) (0.6 wt% B). The catalyst was not calcined after the impregnation of Co.

The HDS activity of the catalysts decreased in the order CVD-Co/Co-MoS_2/BAl(cal) > CVD-Co/Co-MoS_2/Al(cal) > Co-MoS_2/Al(cal) ≅ Co-MoS_2/BAl(cal) in the whole range of Co loadings.

Fig. 3 depicts the HDS activity of the uncalcined catalysts as a function of Co loading. Irrespective of the addition of boron, the HDS activity of Co-MoS_2/Al_2O_3(unc) catalysts increased as the Co loading was increased up to 4 wt%, followed by a very slight decrease with further addition of Co. The HDS activities of the Co-MoS_2(unc) catalysts were unchanged by the addition of boron. A comparison of the activities of Co-MoS_2(cal) (Fig. 2) and Co-MoS_2(unc) (Fig. 3) shows that calcination af-

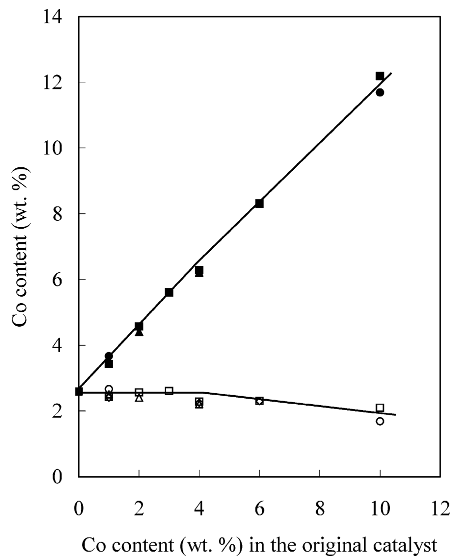

Fig. 4. Amounts of Co in CVD-Co/Co-MoS_2/(B)Al as a function of Co content in the original catalyst. (●) CVD-Co/Co-MoS_2/Al(cal), (■) CVD-Co/Co-MoS_2/Al(unc), (▲) CVD-Co/Co-MoS_2/BAl(cal), (◆) CVD-Co/Co-MoS_2/BAl(unc). Closed symbols, total amount of Co in CVD-Co/Co-MoS_2/(B)Al; open symbols, incremental amount of Co in CVD-Co/Co-MoS_2/(B)Al.

ter the addition of Co slightly increased the HDS activity. The HDS activities of Co-MoS_2/Al(unc) and Co-MoS_2/BAl(unc) were increased by the addition of Co using the CVD technique, as shown in Fig. 3. However, the activity increase was observed only below 3 wt% Co, and the activity of CVD-Co/Co-MoS_2/(B)Al(unc) significantly decreased as the Co content in the impregnation catalyst was increased up to 3 wt%, in sharp contrast to the activity behavior of the calcined counterparts shown in Fig. 2.

The Co content of the CVD-Co/Co-MoS_2/(B)Al catalyst and the additional Co content resulting from the CVD technique (i.e., the difference in Co content between CVD-Co/Co-MoS_2/(B)Al and Co-MoS_2/(B)Al) are shown in Fig. 4 as a function of the Co content in Co-MoS_2/(B)Al. It is obvious that virtually the same amount of Co was anchored by using $Co(CO)_3NO$, irrespective of the original Co content in Co-MoS_2/Al, the addition of boron, and calcination, except for the catalysts with >4 wt% Co, in which a slightly decreasing amount of Co is anchored with increasing Co content.

3.2. *Magnetic properties of Co in Co-MoS_2/Al*

We characterized Co-MoS_2/Al(unc) by means of magnetic properties. The magnetic susceptibility of Co-MoS_2/Al(unc) showed an antiferromagnetic behavior characteristic of the Co-Mo-S phase, in agreement with our previous study [27]. When we assume the formation of a dinuclear unit of two Co atoms (a spin pair model), the magnetic susceptibility χ of Co can be expressed by [26]

$$\chi = \alpha N_A g^2 \mu_B^2 / k_B T\big[3 + \exp(-2J/k_B T)\big], \tag{1}$$

where N_A is the Avogadro constant; μ_B is the Bohr magneton; g is the gyromagnetic factor (assumed to be 2.0 here); k_B is the Boltzmann constant; J is the magnetic interaction strength defined by $H = -2JS_1S_2$; and α is the fraction of the paramagnetic spin per Co atom or the fraction of the Co atoms forming the Co-Mo-S phase in the total amount of Co in the sample. Table 1 summarizes the fitting parameters, J, and α values for Co-MoS_2/Al(unc). The α values are around 0.8, indicating that about 80% of Co atoms form the Co-Mo-S phase, whereas about 20% of Co atoms are present as Co_9S_8-like cobalt sulfide clusters at a Co content of 0.77–3.08 wt%.

Table 1
Magnetic parameters obtained by fitting the experimental magnetic susceptibility of Co assuming dinuclear Co clusters on the edge of MoS_2 particles of Co-MoS_2/Al(unc)

Co content (wt% Co)	J (K)	α
0.77	−5.0	0.80
1.54	−5.3	0.83
2.31	−5.6	0.94
3.08	−5.6	0.80

The J value for a SiO_2-supported CVD-Co/MoS_2 catalyst, which showed 1.6 times higher intrinsic activity than Al_2O_3-supported counterparts for the HDS of thiophene [21], was −8.1 K [27]. Accordingly, the value of J is considered to be virtually constant regardless of the Co content, suggesting formation of the identical type of the Co-Mo-S phase in the catalysts.

3.3. *DRS UV–vis spectra*

The diffuse UV–vis reflectance spectra for the oxidic catalysts after calcination at 773 K for 5 h show an intense triplet at 550, 590, and 640 nm (Fig. 5), characteristic of Co^{2+} ions in a tetrahedral coordination as found in $CoAl_2O_4$ [20,28]. The intensity of the peaks increased with increasing Co content (Fig. 5), indicating that the amount of $CoAl_2O_4$-like Co species increases with increasing Co content, irrespective of the addition of boron, as expected. Obviously, the addition of boron decreased the intensity of the triplet peaks, reflecting a decrease in the amount of $CoAl_2O_4$-like Co species. The band due to octahedral Co^{2+} ions that are supposed to appear at 480 nm [28] was not observed in the present study, because the spectral region is overlapped with the very intense bands due to Co_3O_4. Broad bands due to Co_3O_4 clearly appeared at around 400 and 740 nm [28,29], especially for the 6 wt% CoO-MoO_3 catalysts. Although estimating the relative amounts of $CoAl_2O_4$-like Co^{2+} species and Co_3O_4, is quite difficult, the weakened triplet and clearer shoulder at 740 nm in the spectra for the boron-added catalysts may suggest an increased contribution of Co_3O_4 from the addition of boron, in contrast to the suggestion by Stranick et al. [20] that with Co/Al_2O_3 calcined at 873 K, addition of boron increased the amount of Co^{2+} in an octahedral coordination and decreased the amounts of $CoAl_2O_4$-like Co^{2+} species and Co_3O_4.

4. Discussion

The addition of about 0.6 wt% of boron enhanced the HDS activity of CVD-Co/MoS_2/Al and (slightly) CVD-Co/Co-

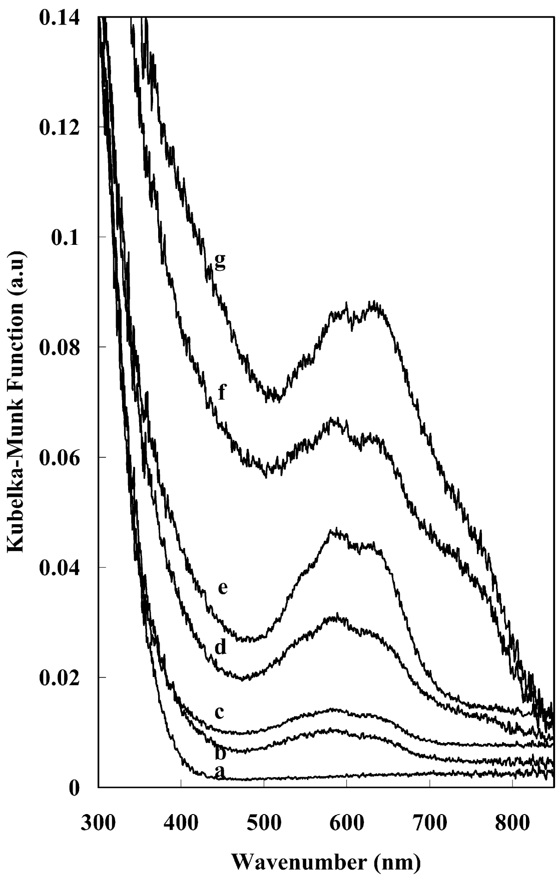

Fig. 5. UV-visible spectra of (a) MoO_3/Al, (b) 1 wt% Co/MoO_3/BAl, (c) 1 wt% Co/MoO_3/Al, (d) 4 wt% Co/MoO_3/BAl, (e) 4 wt% Co/MoO_3/Al, (f) 6 wt% Co/MoO_3/BAl, and (g) 6 wt% Co/MoO_3/Al. All the catalysts were calcined at 773 K for 5 h.

Table 2
Structural parameters and HDS activity of 4 wt% Co-MoS_2 catalysts

Catalyst	θ_{Co}	Φ_b	Φ_{CoMoS}	HDS activity (mmol g^{-1} h^{-1})	TOF (h^{-1})
CVD-Co/MoS_2/Al[a]	1.00	0.00	1.00	3.75	8.4
CVD-Co/MoS_2/BAl[b]	1.00	0.00	1.00	4.35	10.6
Co-MoS_2/Al(cal)	0.91	0.13	0.59	3.01	
CoMoS_2/Al(unc)	1.00	0.32	0.72	2.74	
CoMoS_2/BAl(cal)	0.76	0.19	0.46	2.87	
CoMoS_2/BAl(unc)	1.00	0.40	0.69	2.70	

θ_{Co}: Fractional Co coverage on MoS_2 edge sites.
Φ_b: Extent of blocking of MoS_2 edges site.
Φ_{CoMoS}: Fraction of Co atoms forming the Co-Mo-S phase.
[a] Co content = 2.60 wt% Co.
[b] Co content = 2.41 wt% Co.

MoS_2/Al (Figs. 1 and 2), in good agreement with our previous studies [17,18,25]. This is due to weakened surface interactions between MoS_2 and Al_2O_3 support by the addition of boron, resulting in a shift of the type of Co-Mo-S active sites from Co-Mo-S type I to Co-Mo-S (pseudo) type II [25], in agreement with a higher TOF on CVD-Co/MoS_2/BAl than that on CVD-Co/MoS_2/Al (Table 2). However, at a higher boron content, the dispersion of MoS_2 particles on the surface of Al_2O_3 is decreased [17,25], resulting in decreased HDS activity, as shown in Fig. 1.

However, under the present experimental conditions, the addition of boron rarely changed the apparent performance of Co-MoS_2/Al in the HDS of thiophene at low boron content (0.6 wt% B) irrespective of the calcination and Co loading (Figs. 1–3). This is in line with the results of Lewandosky and Sarbak [13], who reported that the addition of boron did not affect the activity of Ni-Mo/Al_2O_3 catalysts for the HDS of coal liquid. In contrast, Ramirez et al. [16] reported that the addition of boron significantly increased the thiophene HDS activity of Co-Mo/Al_2O_3 catalysts. These contradictory results may be due to differences in preparation methods and reaction conditions producing differences in catalyst surface structure.

Several parameters determine the HDS activity of Co-Mo catalysts, including dispersion of MoS_2 on the surface of support, Co coverage on the edges of MoS_2 particles, blocking of MoS_2 edges by catalytically inactive cobalt sulfide clusters, and type of Co-Mo-S active phase. The dispersion of MoS_2 particles was not significantly modified by the addition of Co using the double-impregnation process and by the addition of 0.6 wt% boron, as shown in Fig. 4. Therefore, the change in the HDS activity in Figs. 2 and 3 is considered not correlated with the change in the dispersion of MoS_2 particles, except for Co-MoS_2/BAl with an excess amount of boron, in which the dispersion of MoS_2 particles is considerably decreased [17,25]. The change of the HDS activity in the present study can then be correlated with the Co coverage on the edges of MoS_2 particles, the blocking of MoS_2 edges by catalytically inactive cobalt sulfide clusters, and the type of the Co-Mo-S structure.

In the calculations of the extent of blocking of MoS_2 edges by cobalt sulfide clusters and of the fractional coverage of Co on MoS_2 edges on the basis of the HDS activity of the catalysts, we assume that the HDS activity is proportional to the number of the active sites, the Co-Mo-S phase. It is rational to assume a proportional correlation between them if the intrinsic activity of the Co-Mo-S phase is independent of the coverage of Co on the MoS_2 edges. It is most likely that this prerequisite is usually fulfilled in Co-Mo sulfide catalysts, because linear correlations have been reported between the number of the Co atoms in the Co-Mo-S phase and the HDS activity or rate constant [5,30]. The magnetic properties of Co-MoS_2/Al_2O_3(unc) substantiate the prerequisite that the J value, which is correlated with the Co-Co electronic interaction strength in a dinuclear Co-Mo-S structure [27] and to the intrinsic activity of the structure [31], is independent of the Co content below 3 wt% Co (Table 1). Therefore, it is safe to evaluate the surface structure of Co-MoS_2 catalysts on the basis of the HDS activity in conjunction with the CVD technique using $Co(CO)_3NO$ as a probe molecule.

4.1. Effect of boron addition on the extent of blocking of MoS_2 edges

It is apparent from Figs. 1–3 that the HDS activity of CVD-Co/MoS_2/(B)Al is higher than that of Co-MoS_2/(B)Al or CVD-Co/Co-MoS_2/(B)Al, because the edges of MoS_2 particles are fully covered by the Co atoms in the Co-Mo-S phase in the CVD catalysts. In this study, therefore, we used CVD-

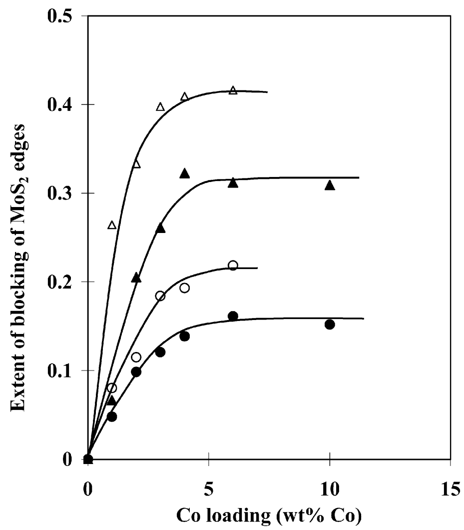

Fig. 6. Extent of blocking of MoS_2 edge sites as a function of Co loading. (●) Co-MoS_2/Al(cal), (○) Co-MoS_2/BAl(cal), (▲) Co-MoS_2/Al(unc), (△) Co-MoS_2/BAl(unc).

Co/MoS_2/(B)Al as the maximum potential activity catalyst [22,23]. When Co atoms were added by an impregnation technique (Co-MoS_2/Al_2O_3), part of the Co atoms formed catalytically inactive cobalt sulfide clusters and blocked the edge sites of MoS_2 particles [23]. The existence of cobalt sulfide clusters over Co-MoS_2/Al_2O_3 (4 wt% Co) was demonstrated previously by means of XANES analysis [23], in agreement with the Mössbauer emission spectroscopy study by Wivel et al. [32]. The lower HDS activity of CVD-Co/Co-MoS_2/(B)Al compared with the maximum potential activity is then ascribed to the blocking of MoS_2 edges by catalytically inactive cobalt sulfide clusters.

We can estimate the extent of blocking of MoS_2 particles (Φ_b) in the Co-MoS_2/(B)Al catalysts on the basis of the HDS activities of CVD-Co/Co-MoS_2/(B)Al and CVD-Co/MoS_2/(B)Al in Figs. 1–3,

$$[\text{Co/Co-MoS}_2] = [\text{Co/MoS}_2](1 - \Phi_b). \quad (2)$$

We then have

$$\Phi_b = \big([\text{Co/MoS}_2] - [\text{Co/Co-MoS}_2]\big)/[\text{Co/MoS}_2], \quad (3)$$

where [Co/MoS_2] and [Co/Co-MoS_2] represent the activities of CVD-Co/MoS_2/(B)Al (the maximum potential activity) and CVD-Co/Co-MoS_2/(B)Al, respectively. The extent of the blocking linearly increased as the Co content was increased below ca. 2 wt% Co (Fig. 6), increased more gradually up to ca. 4 wt% Co, and remained almost constant with further increases in Co content, irrespective of the calcination and the addition of boron. The extent of blocking increased in the order Co-MoS_2/Al(cal) < Co-MoS_2/BAl(cal) < Co-MoS_2/Al(unc) < Co-MoS_2/BAl(unc).

Based on their Mössbauer emission spectroscopy and XAFS studies of supported Co-Mo catalysts, Crajé et al. [33–35] and van der Kraan et al. [36] proposed a sophisticated surface model of Co-Mo catalysts in which highly-dispersed cobalt-sulfide particles are located at the edge positions of MoS_2 crystallites and the size of the cobalt sulfide particles increases as the Co/Mo ratio increases. Consistent with their surface model, we also consider the formation of cobalt sulfide clusters in contact with MoS_2 particles. Their studies assumed a catalytic synergy between the cobalt sulfide clusters and molybdenum sulfide [33–36], in contrast to the active site blocking by the cobalt sulfide clusters in the present study. The increase in the extent of blocking with increasing Co content is a consequence of the increasing size and number of the cobalt sulfide clusters.

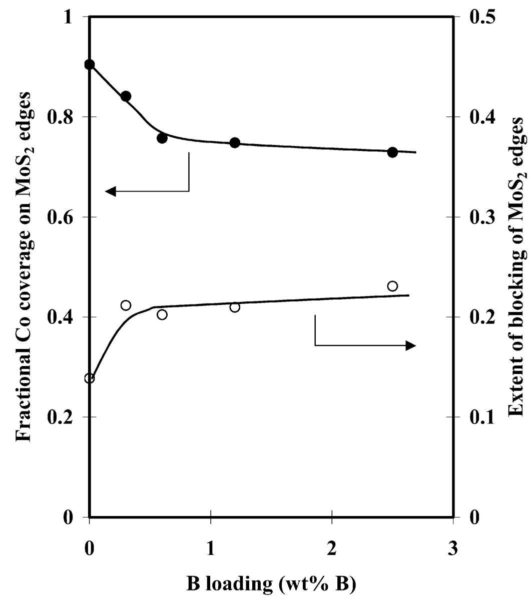

Fig. 7. (●) Fractional Co coverage on MoS_2 edge sites and (○) the extent of blocking of MoS_2 edges for 4 wt% Co-MoS_2/BAl(cal) as a function of boron loading.

The extent of blocking of MoS_2 edges for 4 wt% Co-MoS_2/BAl(cal) was significantly increased by the addition of 0.3 wt% boron, followed by a very slight increase with a further addition of boron. These results suggest that the addition of boron increases the extent of blocking of MoS_2 edge sites by catalytically inactive species, in contrast to calcination, which decreases the extent of the blocking.

Fig. 5 suggests that the addition of boron reduces the fraction of tetrahedrally coordinated Co species. In line with this, Stranick et al. [20] have reported that the boron in B_2O_3-Al_2O_3 occupies the tetrahedral sites on Al_2O_3 surface; therefore, the addition of boron retards the formation of Co atoms in the alumina matrix. Thus, the addition of boron may decrease the dispersion of Co atoms by promoting the formation of Co_3O_4, the precursor of Co_9S_8 [5,32], thereby increasing the number of Co atoms forming Co_9S_8 and decreasing the amount of the Co-Mo-S phase.

As shown in Fig. 7, a very small amount of boron (<0.6 wt%) significantly affected the extent of blocking. The number of boron atoms in 0.6 wt% B (1.85 B/nm^2) is approximately equivalent to the number of Co atoms in 3 wt% Co. Thus, a boron content of 0.6 wt% is sufficient to remove Co^{2+}-Al_2O_3 interaction sites, and further addition of boron affects the Co-Al_2O_3 interactions only slightly but significantly weakens the Mo oxide-Al_2O_3 interactions by consuming the basic surface OH groups [18,25].

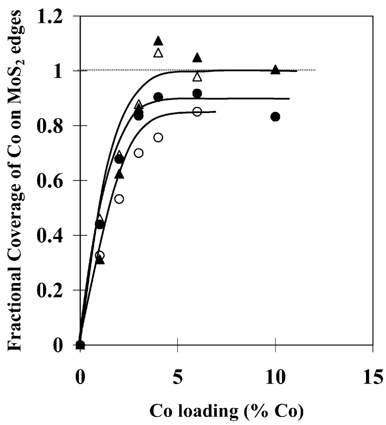

Fig. 8. Fractional coverage of Co on MoS_2 edges as a function of Co loading. (●) Co-MoS_2/Al(cal), (○) Co-MoS_2/BAl(cal), (▲) Co-MoS_2/Al(unc), (△) Co-MoS_2/BAl(unc).

4.2. *Effect of boron addition on Co coverage on MoS_2 edges*

In the present study, we calculated the fraction of coverage of Co on MoS_2 edge sites on the basis of the maximum potential activity of the catalysts. The Co coverage on MoS_2 edges (θ_{Co}) was calculated using the following equation:

$$\begin{aligned}[\text{Co-MoS}_2] &= [\text{Co/MoS}_2]\theta_{Co}(1-\Phi_b) \\ &\quad + [\text{MoS}_2](1-\theta_{Co})(1-\Phi_b) \\ &= [\text{Co/Co-MoS}_2]\theta_{Co} + [\text{MoS}_2](1-\theta_{Co})(1-\Phi_b).\end{aligned} \tag{4}$$

Then

$$\begin{aligned}\theta_{Co} &= \big([\text{Co-MoS}_2] - [\text{MoS}_2](1-\Phi_b)\big) \\ &\quad \big/\big([\text{Co/Co-MoS}_2] - [\text{MoS}_2](1-\Phi_b)\big),\end{aligned} \tag{5}$$

where [Co-MoS_2] and [MoS_2] represent the HDS activities of Co-MoS_2/(B)Al and MoS_2/(B)Al, respectively. In Eqs. (4) and (5), it is assumed that the MoS_2 edges occupied and unoccupied by Co atoms are equally blocked by catalytically inactive cobalt sulfide species. The second term of the right side of Eq. (4) shows the contribution of the HDS activity from unblocked Co-free MoS_2 edges. The HDS activity of cobalt sulfide clusters is neglected here.

Fig. 8 depicts the fractional coverage of Co on MoS_2 edges thus estimated from Eq. (5) as a function of Co content. The coverage increased as the cobalt content was increased up to 4 wt% Co and remained almost constant with a further increase of Co content up to 10 wt%, irrespective of the addition of boron and calcination. As for the calcined catalysts, the maximum Co coverage on MoS_2 edges was ca. 90% for Co-MoS_2/Al and 80% for Co-MoS_2/BAl. Vacant sites on the MoS_2 edge sites exist on Co-MoS_2/Al(cal) even at a high Co content, in line with our previous study [23]. In parallel with this, by using FTIR spectra of NO adsorption, Topsøe and Topsøe [37] observed the doublet bands due to NO adsorption on Mo sites even at a high Co content on their sulfided Co-Mo/Al_2O_3 impregnation catalysts.

The fractional coverage of Co on the edges of MoS_2 particles is illustrated in Fig. 7 for Co-MoS_2/BAl(cal) as a function

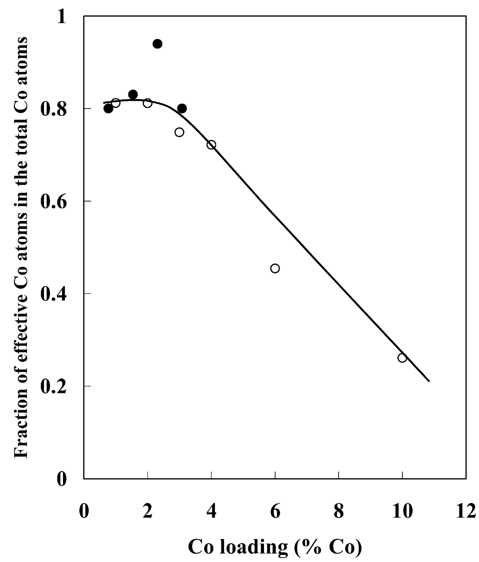

Fig. 9. Fraction of Co atoms forming the Co-Mo-S phase over Co-MoS_2/Al(unc). (○) Calculated from the Co coverage of MoS_2 edges (Φ_{CoMoS}) and (●) calculated from magnetic properties.

of the boron content. The addition of boron up to 0.6 wt% significantly decreased the fractional coverage of Co, followed by a very slight decrease with a further addition of boron up to 2.5 wt%. This is due to an increased amount of cobalt sulfide clusters as a consequence of a decreased dispersion of Co and an increased amount of Co_3O_4 (Fig. 5). Part of the resultant cobalt sulfide clusters blocks the Co-Mo-S phase.

4.3. *Fraction of Co atoms forming the Co-Mo-S structure*

It is well established that Co atoms in commercial catalysts are present in several kinds of chemical states, e.g., $CoAl_2O_4$-like Co^{2+} and Co_9S_8 clusters as well as the Co-Mo-S phase [5]. Since only the Co atoms in the Co-Mo-S phase form catalytically active sites [5,8,9], it is of great importance to investigate the percentage of the Co atoms which form the Co-Mo-S phase in the total amount of Co atoms in the impregnation catalysts as a function of the preparation parameter. We designate the Co atoms forming the Co-Mo-S phase as an "effective" Co. The fraction of the effective Co (Φ_{CoMoS}) was calculated by the following equation:

$$\Phi_{CoMoS} = (\text{Co-CVD})\theta_{Co}/(\text{Co-imp}), \tag{6}$$

where (Co-CVD) and (Co-imp) represent the amounts of Co atoms in CVD-Co/MoS_2/(B)Al (the maximum potential activity catalyst) and in Co-MoS_2/(B)Al, respectively. In Eq. (6), it is assumed that the MoS_2 edges blocked by cobalt sulfide clusters are also covered by the Co-Mo-S phase at a coverage of θ_{Co}.

Fig. 9 shows the fraction of effective Co (Φ_{CoMoS}) for Co-MoS_2/Al(unc) as a function of Co loading. The α values, the empirical fraction of the Co atoms in the Co-Mo-S phase, in Table 1 are also plotted in Fig. 9, showing an excellent agreement with the calculation results. As shown in Fig. 9, only about 80% of Co atoms in Co-MoS_2/Al(unc) form the Co-Mo-S phase below 3 wt% Co, whereas about 20% forms cobalt sulfide clusters even at a very low loading of Co (0.77 wt%). This means that cobalt sulfide clusters are simultaneously formed together with the Co-Mo-S phase rather than no more vacant sites available on MoS_2 edges.

4.4. Surface structure of Co-MoS$_2$/Al

The structural parameters of 4 wt% Co-MoS_2 catalysts (Co/Mo = 0.75), as well as the activity for the HDS of thiophene, are summarized in Table 2. The uncalcined catalyst showed lower HDS activity than the calcined catalyst, despite the greater number of Co atoms in the Co-Mo-S phase. This is apparently due to a severe blocking of the Co-Mo-S phase in Co-MoS_2(unc), which is partly removed by calcination. Calcination increases the dispersion of Co due to enhanced interactions between Co and Al_2O_3 and Mo phases in the oxidic state [5]. The addition of boron did not lead to increased HDS activity in the present catalyst preparations. The increased intrinsic activity of the Co-Mo-S phase was compensated for both by the decreased θ_{Co} and increased Φ_b for Co-MoS_2/BAl(cal) due to the increased amount of Co_3O_4 resulting from the addition of boron.

Poor Co dispersion in the oxidic state has two detrimental effects on the performance of HDS catalysts. First, the number of Co cations (e.g., in octahedral coordinations [5] favorable for the formation of the Co-Mo-S phase) decreases. Second, the resultant cobalt sulfide clusters block the Co-Mo-S phase, resulting in a further decrease in the active phase available to reactants.

5. Conclusions

The salient findings in the present study can be summarized as follows:

1. The addition of boron (0.6 wt% B) hardly changed the performance of Co-Mo/Al_2O_3 catalysts for the HDS of thiophene under the present experimental conditions.
2. The addition of boron increased the extent of blocking and decreased the fraction of Co coverage on the MoS_2 edges, irrespective of the Co loading.
3. Calcination reduced both the blocking of MoS_2 edges by cobalt sulfide clusters and the Co coverage on the MoS_2 edges, irrespective of the addition of boron.
4. The magnetic property of the Co-Mo-S phase is independent of the coverage of Co on the MoS_2 edges.

Acknowledgment

This work was supported by a Grant-in-Aid for Scientific Research (16360404) from the Japanese Ministry of Education, Culture, Sport, Science, and Technology.

References

[1] C. Song, Catal. Today 86 (2003) 211.
[2] C. Song, X. Ma, Appl. Catal. B 41 (2003) 207.
[3] K.G. Knudsen, B.H. Cooper, H. Topsøe, Appl. Catal. A 189 (1999) 205.
[4] R. Prins, in: G. Ertl, H. Knözinger, H.J. Weitkamp (Eds.), Handbook of Heterogeneous Catalysis, VCH, Weinheim, 1997, p. 1908.
[5] H. Topsøe, B.S. Clausen, F.E. Massoth, in: J.R. Anderson, M. Boudard (Eds.), Catalysis Science and Technology, vol. 11, Springer-Verlag, Berlin, 1996.
[6] T. Kabe, A. Ishihara, W. Qian, Hydrodesulfurization and Hydrodenitrogenation, Kodansha, Tokyo, 1999.
[7] D.D. Whitehurst, T. Isoda, I. Mochida, Adv. Catal. 42 (1998) 345.
[8] R. Candia, O. Sørensen, J. Villadsen, N.-Y. Topsøe, B.S. Clausen, H. Topsøe, Bull. Soc. Chim. Belg. 93 (1984) 763.
[9] H. Topsøe, B.S. Clausen, Catal. Rev. Sci. Eng. 26 (1984) 395.
[10] S. Eijsbouts, Appl. Catal. A 158 (1997) 53.
[11] Y. Okamoto, A. Kato, Usman, K. Sato, T. Kubota, Chem. Lett. 34 (2005) 1258.
[12] D. Li, T. Sato, M. Imamura, H. Shimada, A. Nishijima, Appl. Catal. B 16 (1998) 255.
[13] M. Lewandowski, Z. Sarbak, Fuel 79 (2000) 487.
[14] D. Ferdous, A.K. Dalai, J. Adjaye, Appl. Catal. A 260 (2004) 153.
[15] Y.W. Chen, M.C. Tsai, Catal. Today 50 (1999) 57.
[16] J. Ramírez, P. Castillo, L. Cedeño, R. Cuevas, M. Castillo, J.M. Palacios, A.L. Agudo, Appl. Catal. A 132 (1995) 317.
[17] Usman, T. Kubota, Y. Araki, K. Ishida, Y. Okamoto, J. Catal. 227 (2004) 523.
[18] Usman, M. Takaki, T. Kubota, Y. Okamoto, Appl. Catal. 286 (2005) 148.
[19] H. Morishige, Y. Akai, Bull. Soc. Chim. Belg. 104 (1995) 4.
[20] M.A. Stranick, M. Houalla, D.M. Hercules, J. Catal. 104 (1987) 396.
[21] Y. Okamoto, K. Ochiai, M. Kawano, K. Kobayashi, T. Kubota, Appl. Catal. A 226 (2002) 115.
[22] Y. Okamoto, S. Ishihara, M. Kawano, M. Satoh, T. Kubota, J. Catal. 217 (2003) 12.
[23] Y. Okamoto, K. Ochiai, M. Kawano, T. Kubota, J. Catal. 222 (2004) 143.
[24] Y. Okamoto, T. Kubota, Catal. Today 86 (2003) 31.
[25] Usman, T. Kubota, Y. Okamoto, Bull. Chem. Soc. Jpn. 79 (2006) 637.
[26] O. Kahn, Molecular Magnetism, VCH, Weinheim, 1993, chap. 6.
[27] Y. Okamoto, M. Kawano, T. Kawabata, T. Kubota, I. Hiromitsu, J. Phys. Chem. B 109 (2005) 288.
[28] L.F. Liotta, G. Pantaleo, A. Macaluso, G. Di Carlo, G. Deganello, Appl. Catal. A 245 (2003) 167.
[29] M.J.M. van der Aalst, V.H.J. de Beer, J. Catal. 49 (1977) 247.
[30] F. Maugé, A. Vallet, J. Bachelier, J.C. Duchet, J.C. Lavalley, J. Catal. 162 (1996) 88.
[31] Y. Okamoto, A. Kato, Usman, K. Sato, I. Hiromitsu, T. Kubota, J. Catal. 233 (2005) 16.
[32] C. Wivel, R. Candia, B.S. Clauses, S. Mørup, H. Topsøe, J. Catal. 68 (1981) 453.
[33] M.W.J. Crajé, S.P.A. Louwers, V.H. J de Beer, R. Prins, A.M. van der Kraan, J. Phys. Chem. 96 (1992) 5445.
[34] M.W.J. Crajé, V.H.J. de Beer, A.M. van der Kraan, Appl. Catal. 70 (1991) L7.
[35] M.W.J. Crajé, V.H.J. de Beer, A.M. van der Kraan, Bull. Soc. Chim. Belg. 100 (1991) 983.
[36] A.M. van der Kraan, M.W.J. Crajé, E. Gerkema, W.L.T.M. Ramselaar, V.H.J. de Beer, Hyperfine Interact. 46 (1989) 567.
[37] N.Y. Topsøe, H. Topsøe, J. Catal. 75 (1982) 354.